

Supporting Information

Bottom-Up Assembly of DNA–Silica Nanocomposites into Micrometer-Sized Hollow Spheres

*Yong Hu, Maximilian Grösche, Sahana Sheshachala, Claude Oelschlaeger, Norbert Willenbacher, Kersten S. Rabe, and Christof M. Niemeyer**

anie_201910606_sm_miscellaneous_information.pdf

Experimental Section

Materials. Tetraethyl orthosilicate (TEOS), 3-(trihydroxysilyl)propyl methylphosphonate (THPMP, monosodium salt solution), (3-aminopropyl)trimethoxysilane (APTMS), poly(ethylene glycol) methyl ether maleimide (mPEG-mal, molecular weight of ~2000), N1-(3-trimethoxysilylpropyl)diethylenetriamine (DETAPTMS), tris(2-carboxyethyl)phosphine hydrochloride (TCEP, 0.5 M in water), sodium cyanoborohydride, and oligonucleotides were purchased from Sigma-Aldrich. Cyclohexane, 1-hexanol and glutaraldehyde (50% in water) were from VWR. (3-mercaptopropyl) trimethoxysilane (MPTMS) was purchased from Alfa Caesar. Sulfo-cyanine 5 NHS-ester was from Lumiprobe. Triton X-100 and glycine were from AppliChem. 1-palmitoyl-2-oleoyl-sn-glycero-3-phosphocholine (POPC), 1,2-dioleoyl-3-trimethylammonium-propane (DOTAP) (chloride salt) and 1,2-dimyristoyl-sn-glycero-3-phosphoethanolamine-N-(lissamine rhodamine B sulfonyl) (Rh-PE) (ammonium salt) were from Avanti Polar Lipids. Mineral oil was from Carl Roth. All chemicals were used as received without further purification.

Synthesis of multifunctional silica nanoparticles. Multifunctional SiNP (SiNP-1, in Figure S1) with amino, thiol and phosphonate groups and an average particle size of around 80 nm were synthesized according to previous work.^[1] Typically, cyclohexane (38 mL), 1-hexanol (9 mL) and triton X-100 (9 mL) were mixed vigorously in a 250 mL round-bottom glass flask. Double distilled water (2 mL) was added to the mixture to produce stable reverse micelles. After mixing for 10 min, TEOS (500 μ L) was added to the mixture followed by adding ammonia solution (28-30%, 500 μ L). This mixture was stirred at room temperature for 24 h. Subsequently, additional TEOS (250 μ L) was added to the mixture, and after stirring for 30 min, THPMP (200 μ L) and DETAPTMS (50 μ L) were added to modify the surface of the nanoparticles with negatively charged phosphonate and amino groups. The mixture was allowed to react for 24 h and subsequently, MPTMS (30 μ L) was added to modify the nanoparticle's surface with thiol groups. The mixture was stirred at room temperature for an additional 3 h. The micelles were broken with acetone, and the resulting nanoparticles were centrifuged and washed at least 5 times with absolute ethanol, and finally dispersed in PBS buffer (23 mM KH_2PO_4 , 77 mM K_2HPO_4 , 50 mM NaCl, pH 7.4) to a final concentration of 10 mg/mL.

The preparation of Cy5 containing core/shell SiNP-1 was carried out according to previously reported procedures.^[2] In brief, 1.3 μmol sulfo-Cy5-NHS was dissolved in 1 mL of anhydrous DMSO and APTMS was added at a molar ratio of 10:1 APTMS: dye. The mixture was allowed to react at room temperature for 12 h. Subsequently, the crude reaction mixture (200 μL) was transferred into a 250 mL round-bottom glass flask containing stable reverse micelles prepared as described above. The Cy5-doped SiNP were synthesized in the dark by further addition of TEOS, THPMP, DETAPTMS, and MPTMS in the presence of ammonia solution using to the same procedure described above for the preparation of unlabeled **SiNP-1**.

Immobilization of PEG and ssDNA on silica nanoparticles. To install PEG on the surface of **SiNP-1**, TCEP (0.5 M solution, 8.0 μL) was added to a 1 mL PBS solution of **SiNP-1** (10 mg/mL) to reduce any disulfide bonds. Subsequently, a DMSO solution of mPEG-mal (50 mg/mL, 10 μL) was added to the mixture. After incubation at room temperature overnight, PEG-modified nanoparticles were purified by centrifugation and re-dispersion in PBS buffer for 3-5 times. The resulting nanoparticles are denoted as **SiNP-2** (Figure S1).

Next, amino-terminated **Ih** was covalently immobilized on the particle surface *via* glutardialdehyde coupling. Typically, **SiNP-2** (10 mg/mL, 1.0 mL) in PBS buffer were mixed with glutardialdehyde (50 % in water, 250 μL), and the mixture was stirred at room temperature for 1 h. The resulting nanoparticles were washed 3 times with PBS buffer, re-dispersed in PBS buffer (1.0 mL) and mixed with **Ih** (100 μM , 50 μL). The mixture was incubated at room temperature for 12 h. Subsequently, glycine (0.4 M, 1.0 mL) was added to block any unreacted aldehyde groups, followed by addition of sodium cyanoborohydride (60 mM, 400 μL) to reduce Schiff bases into stable secondary amines. The **Ih**-modified SiNP are denoted as **SiNP-Ih**. As a control, the **SiNP-Ic** were synthesized using the same protocol.

The density of DNA oligonucleotides on the particle's surface was determined by the supernatant depletion method. Briefly, the mixture of SiNP and DNA was centrifuged to precipitate SiNP and the amount of unbound DNA molecules in the supernatant was determined by absorbance measurement at 260 nm, using a Agilent Cary 100 UV-Vis spectrophotometer.

Annealing procedure for constructing hairpin structures. To prepare DNA hairpins for the linear HCR and the C-HCR processes, the purchased strands (**h1**, **h2** for linear HCR, and **H1**, **H2**

for C-HCR) were heated at 95 °C for 5 minutes and then quickly quenched by cooling on ice. 1× TAE-Mg²⁺ buffer (40 mM Tris, 20 mM acetic acid, 2 mM EDTA, 12.5 mM Mg²⁺, pH = 8.0) was used to dissolve **H1** and **H2** strands and 5× SSC buffer (750 mM sodium chloride, 75 mM sodium citrate, pH = 7.0) was used for **h1** and **h2** strands.

Polymerization of SiNP in bulk. To amplify the number of initiator sequences required for the C-HCR process, linear HCR amplification was conducted firstly with the **SiNP-Ih**. To this end, **h1** (500 μM, 20 μL in 1× TAE-Mg²⁺ buffer) and **h2** (500 μM, 20 μL in 1× TAE-Mg²⁺ buffer) oligomers were successively added to 20 μL **SiNP-Ih** suspension (10 mg/mL in H₂O) and the reaction mixture was incubated at room temperature for 12 h. After purification by centrifugation/resuspension in distilled water for 5 times, the obtained particle suspension was concentrated to 10 μL. Following, the second C-HCR gelation step was carried out by addition of a mixture of **H1** (2.25 mM, 10 μL in 5× SSC buffer) and **H2** (2.25 mM, 10 μL in 5× SSC buffer). The mixture was kept in an open microcentrifuge tube at room temperature for 12 h. Subsequently, 10 μL distilled water were added and the solution was incubated in a closed microcentrifuge tube for another 48 h to obtain the DNA-SiNP nanocomposite hydrogel.

Microfluidic synthesis of DNA-SiNP hollow microspheres. Water-in-oil (W/O) microdroplets were prepared by using a microfluidic flow-focusing T-junction droplet generator chip made of poly(methyl methacrylate) (PMMA), that was fabricated by micromilling, as previously reported.^[3] In a typical procedure, positively charged 1,2-dioleoyl-3-trimethylammonium-propane (DOTAP) (chloride salt, Avanti Polar Lipids) lipid was mixed with 1,2-dimyristoyl-sn-glycero-3-phosphoethanolamine-N-(lissamine rhodamine B sulfonyl) (Rh-PE) (Avanti Polar Lipids) lipid (0.1 mol% of total lipid amount) and the mixture was dissolved in mineral oil (Carl Roth) to a concentration of 4 mM by ultrasonication under ice cooling for 90 min. The so-prepared oil was used as the continuous phase that was injected into the two inlets of the flow-focusing T-junction (see Figure 3, main text).

An aqueous buffered solution containing the DNA-SiNP and the DNA hairpin strands was injected into the junction as the dispersed phase. Specifically, the dispersed phase contained **SiNP-Ih** (0.2 mg/mL in H₂O), pre-polymerized with **h1/h2**, as described above, as well as **H1** and **H2** (20 μM each in 5× SSC buffer). The continuous and dispersed phases were injected into

the T-junction droplet generator chip with flow rates of 20 $\mu\text{L}/\text{min}$ and 1 $\mu\text{L}/\text{min}$, respectively. The microfluidically produced W/O droplets were collected on a silicone-coated cover glass (Sigmacote®, Sigma-Aldrich, prepared according to manufacturer's instructions) to prevent the droplets from sticking to the glass surface. As a control, zwitterionic POPC lipid was used instead of the positively charged DOTAP for the preparation of the oil phase.

Encapsulation of cells into the microfluidic W/O droplets. Suspension-adapted FreeStyle™ CHO-S cells (Thermo Fisher Scientific) were grown in FreeStyle™ CHO Expression Medium supplemented to 8 mM L-glutamine (Thermo Fisher Scientific) at densities between 0.05×10^6 and 1.5×10^6 cells/mL, and kept on the shaker platform rotating at 120-135 rpm on an orbital shaker platform (Thermo Fisher Scientific) placed in an incubator (37 °C, 8% CO₂).

Cells pre-stained with Calcein AM (1 μM , 30 min) were adjusted to a density of 2×10^6 cells per mL medium that was supplemented with the C-HCR reaction mixture containing SiNP-**Ih** prepolymerized by **h1/h2**-mediated HCR (0.2 mg/mL) of DNA hairpin oligomers (**H1**, 20 μM ; **H2**, 20 μM). This mixture was applied as the dispersed phase into the T-junction droplet generator chip to produce W/O droplets as described above.

Dynamic light scattering (DLS) and zeta potential measurements. The hydrodynamic size and zeta potential of SiNP were measured at room temperature using a Malvern Zetasizer Nano ZSP equipped with a standard 633 nm laser.

Electrophoresis. All samples (Figure S2) were prepared from the purchased oligonucleotides without further purification. The samples were loaded onto 6% native polyacrylamide gels ($1 \times \text{TAE-Mg}^{2+}$) that were run using a voltage of 120 V for 45 min. Gel staining was achieved with Gel Red (Biotium), according to manufacturer's instructions.

Electron microscopy analysis. Transmission electron microscopy (TEM) analysis was performed using a FEI Titan³ 80-300 electron microscope (FEI Company) at an accelerating voltage of 200 kV, the samples were prepared by placing a drop of the sample solution onto a 200-mesh carbon-coated Cu grid (Plano GmbH), which was then air-dried at room temperature. For scanning electron microscopy (SEM) analysis, the lyophilized DNA-SiNP nanocomposites were coated with 4 nm of platinum using ion beam deposition and resulting specimen were

analyzed with a QUANTA 650-FEG scanning electron microscope (FEI Company) with an accelerating voltage of 5-10 kV.

Rotational rheology. DNA-SiNP nanocomposite hydrogels were loaded onto a Physica MCR501 (Anton Paar) Rheometer with a parallel-plate geometry of diameter 8 mm. Strain sweep tests were performed with the strain ranging from 0.1% to 25% at a fixed frequency of 1 Hz; time-scan tests were performed with a fixed strain of 1% and a frequency of 1 Hz for 5 min; frequency sweep tests were carried out between 0.1 and 100 rads^{-1} at a fixed strain of 1%. All tests were done at 25 °C.

Fluorescence microscopy. Microfluidic droplets were analyzed by CLSM (LSM 880, Zeiss) and the obtained images were analyzed by Zeiss Zen Blue software. At 5 min post formation of the droplet, the fluidity of lipid and DNA-SiNP assemblies was evaluated with fluorescence recovery after photobleaching (FRAP) experiments. To this end, both lipid and DNA-SiNP nanocomposite assemblies were photobleached (bleach radius 15 μm to 20 μm , bleach time 1 min, laser power 100%) and the recovery of fluorescence was recorded every 20 s for lipid and **SiNP-Ic** or every 5 min for samples obtained from **SiNP-Ih**, respectively.

To investigate the kinetics of the DNA-SiNP nanocomposite assembly within DOTAP W/O droplets, the droplets were generated at rather low flow rates (0.1 $\mu\text{L}/\text{min}$ and 4.5 $\mu\text{L}/\text{min}$ for aqueous phase and oil phase, respectively) using the same microfluidic setup as described above. The flow was stopped and a just formed droplet was analyzed in a time series of frames for 10 min with 10 s interval time. The acquired fluorescent images were fed into a Matlab program designed for automatic extraction of droplet fluorescence intensity.^[3] This enabled plotting of fluorescence intensity at the edge of the droplet (I_E) to the expense of intensity in the center (I_C) against time. The half-life ($T_{1/2}$), indicating half of the dispersed DNA-SiNP nanocomposite as deposited at the droplet borders, was determined by mathematical fitting of the normalized I_E/I_C with an asymptotic function ($y=a-bc^x$).

Table S1. DNA sequences

Name	Sequence (5'-3')	Modification
Ih	[AmC12]TTT TTT TTT TTT TTT TTT TTC ATC TCA GTC TAG GAT TCG GCG TG	5'Amine C12
Ic	[AmC12]TTT TTT TTT TTT TTT TTT TTA CCT CTA TGC ATG AGT CTG CGT GT	5'Amine C12
h1	AGT CTA GGA TTC GGC GTG ACG ACT TTC ACG CCG AAT CCT AGA CTGAGA TG	-
h2	ACA TCG CTA GAG CAC AAT CAC AGG TTA GTC GTC ACG CCG AAT CCTAGA CTT TCA TCT CAG TCT AGG ATT CGG CGT G	-
H1	CTA GAG CAC AAT CAC AGG AGC CAG TTT TCC TGT GAT TGT GCT CTA GCG ATG T	-
H2	GAT CGC GAT CCT GGC TCC TGT GAT TGT GCT CTA GAC ATC GCT AGAGCA CAA TCA CAG G	-

Table S2. Hydrodynamic size, zeta potential and DNA number of SiNP

Name	Hydrodynamic size (nm)	PDI	Zeta potential (mV)	DNA/particle
SiNP	116.6 ± 1.6	0.09 ± 0.05	- 25.2 ± 3.5	N.A. ^a
SiNP-Ic^b	140.2 ± 2.0	0.04 ± 0.02	-39.8 ± 5.4	111.5 ± 6.9
SiNP-Ih	132.6 ± 1.8	0.08 ± 0.02	-37.9 ± 4.2	104.1 ± 13.4

a) Not applicable.

b) Random sequence of Ic was designed not to trigger the linear HCR of h1 and h2.

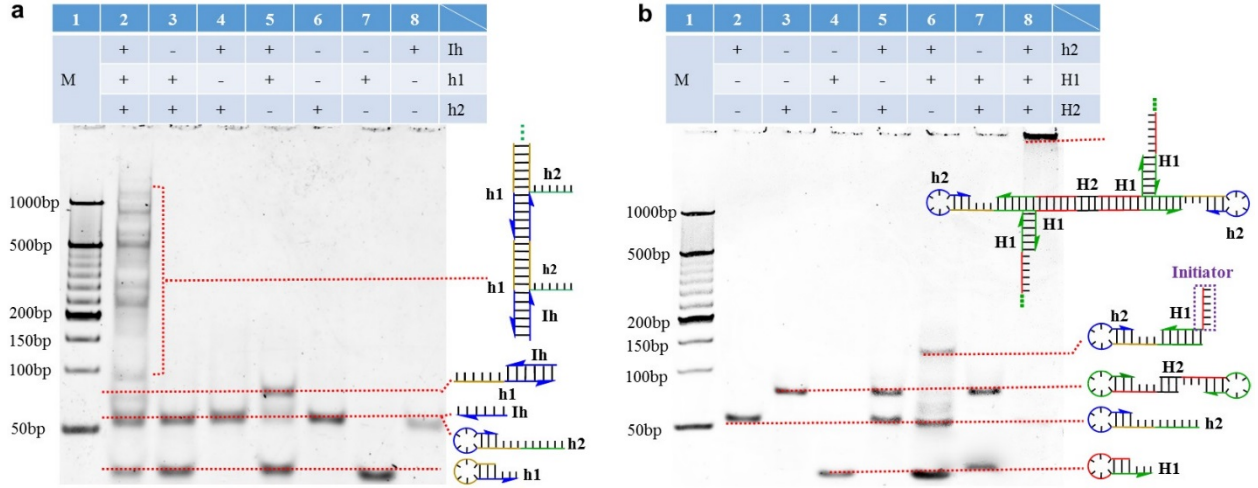


Figure S2. Native polyacrylamide gel electrophoresis (PAGE) analysis of the self-assembly of C-HCR components. Native PAGE analysis of the (a) linear HCR of components **Ih**, **h1**, **h2** and (b) branched C-HCR of components **h2**, **H1**, and **H2**. In **Figure S2a** lanes 6-8 contain single components **h2**, **h1**, and **Ih**, respectively, which appear as single bands. In lane 5, hybridization of **Ih** with **h1** is indicated by formation of a new band with lower electrophoretic mobility. No hybridizations take place between **Ih** and **h2** (lane 4), and **h1** and **h2** (lane 3). In contrast, the mixture of **Ih**, **h1**, and **h2** (lane 2) yields several new bands, thus indicating formation of polymerized hybridization products of different length. In **Figure S2b**, lanes 2-4 contain single components **h2**, **H2** and **H1**, respectively, which appear as single bands. Note that **H1** and **H2** have nearly the same length (52 and 58 nt for **H1** and **H2**, respectively, see Table S1) but **H2** (lane 3) shows a lower electrophoretic mobility than **H1** (lane 4) due to formation of **H2**-dimer, similar as previously described.^[4] No hybridization takes place between **h2** and **H2** (lane 5), or **H1** and **H2** (lane 7), whereas the mixture of excess **H1** with a small amount of initiator **h2** (**H1**:**h2**=50:1) leads to formation of a new band with lower electrophoretic mobility (lane 6). The mixture of all three components leads to the formation of high molecular weight polymers that cannot migrate into the gel (lane 8, **h2**:**H1**:**H2**=1:50:50). Lane M contains DNA molecular weight marker. All samples were incubated at room temperature overnight and then analyzed with 6% native PAGE.

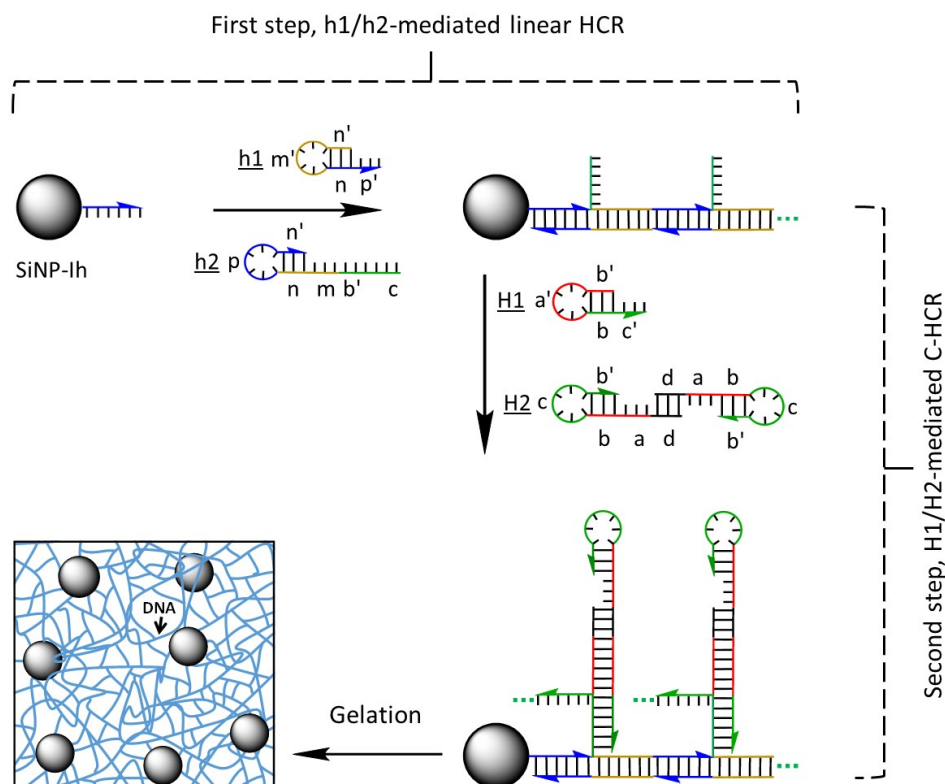


Figure S3. Two-step C-HCR polymerization of initiator modified SiNP.

H2 is a unique component for C-HCR since it has 10 palindromic bases at the 5' end (segment d). After annealing (5 minutes heating at 95 °C and subsequent 2 minutes quenching on ice), two **H2** strands form a hairpin-dimer through the palindromic hybridization.^[4] Hairpin strands **h1** and **h2** or **H1** and **H2**-dimer coexist metastably in the absence of initiators (see also **Figure S2**), since long stems (n/n': 19 bases in **h1** and 18 bases in **h2**, or, b/b': 18 bases in **H1** and **H2**) avoid short loops (m': 6 bases in **h1** and p: 8 bases in **h2**, or, a': 8 bases in **H1** and c: 6 bases in **H2**) to hybridize with toeholds (p' in **h1** and m in **h2**, or, c' in **H1** and a in **H2**). Hence, the pre-polymerization serves to generate more starting points for C-HCR-based gelation and crosslinking. Please note that this explanation corresponds to the one given in the original paper.^[4]

Once **SiNP-Ih** were modified with linear chains by hybridization with **h1** and **h2** through linear HCR, the resulting **SiNP-Ih-h1-h2** were purified and allowed to react with a mixture of **H1** and **H2**-dimer. The single-stranded b'-c segments that protrude from the linear chains on the SiNP act as initiator that first binds to the toehold region of **H1** and opens the long stem and short loop through DNA strand displacement. Next, the so-activated **H1** opens and activates the **H2** through the same mechanism. Then the latter can open another **H1** to repeat this reaction sequence. Importantly, since one **H2**-dimer has two branches, it can form a four-arm junction (with two **H1**) to enable downstream divergent hybridization chain reactions and crosslinking of polyvalent DNA-SiNP. These processes finally lead to gelation by formation of clamped 3D networks, comprising DNA-SiNP and polymeric DNA hydrogels. Please note that this explanation corresponds to the one given in the original paper.^[4]

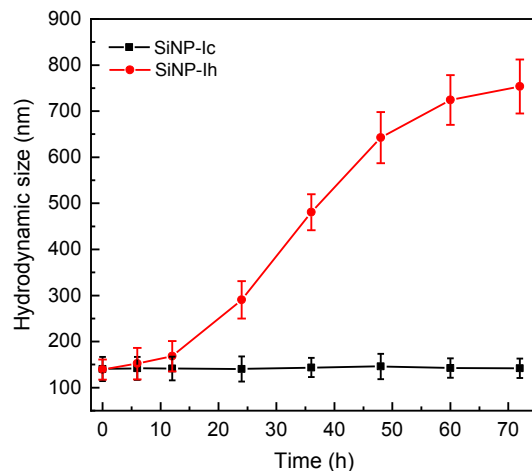


Figure S4. Time-dependent increase in hydrodynamic diameter, determined at 25 °C by DLS. After linear HCR by adding **h1** (500 μ M, 20 μ L) and **h2** (500 μ M, 20 μ L) to **SiNP-Ih** (10 mg/mL, 20 μ L), the purified products (in 300 μ L water) were mixed with **H1** (300 μ M, 100 μ L) and **H2** (300 μ M, 100 μ L) and the increase in hydrodynamic diameter was monitored at 25 °C by DLS. As a control, **SiNP-Ic** were used bearing a random ssDNA sequence (see Table S1).

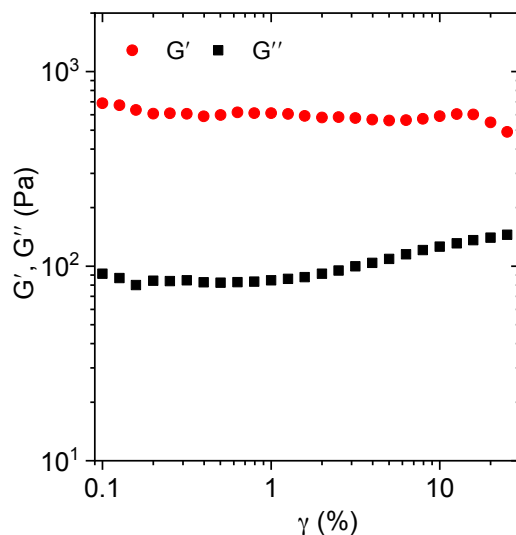


Figure S5. Characterization of the rheological properties DNA-SiNP nanocomposites. A strain sweep test was performed with the strain ranging from 0.1% to 25% at a fixed frequency of 1 Hz. Note that, the storage modulus (G') is constantly higher than the loss modulus (G'') in the entire measurement series at the various strain loads, indicating the structural stability of the polymeric network during rotational measurements (see also, **Figures 2c-d**).

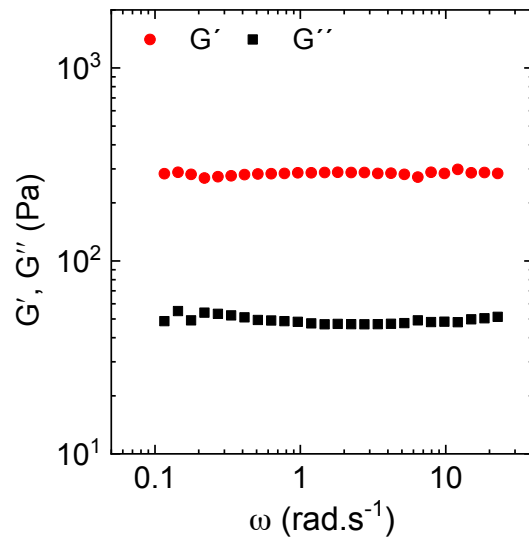


Figure S6. Rheological properties characterization of a pure DNA hydrogel. Frequency sweep test between 0.1 and 20 rad.s^{-1} at a fixed strain of 1%. Note that, during the test, the storage modulus (G') is constantly higher than the loss modulus (G''). The constant elastic modulus was determined as $G_0 \approx 280$ Pa in the given frequency range.

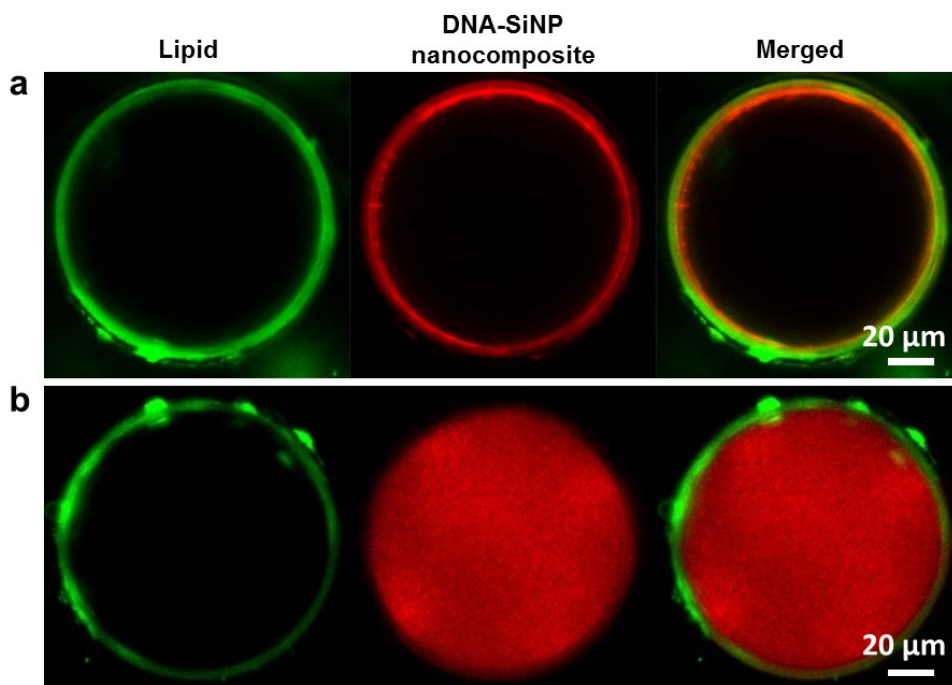


Figure S8. Fluorescence images of DOTAP and POPC W/O droplets encapsulating DNA-SiNP nanocomposite. Representative fluorescence images of (a) DOTAP and (b) POPC W/O droplets encapsulating DNA-SiNP nanocomposite. The lipid membrane and SiNP-Ih are labeled in green and red, respectively. Note that the formation of a DNA-SiNP nanocomposite shell is observed only for W/O droplets prepared with the cationic DOTAP but not with a zwitterionic POPC lipid membrane. Also note that the assembly of the DNA-SiNP nanocomposite inside the DOTAP droplets leads to a distinctive double-layered shell architecture.

Of note, the DNA-SiNP nanocomposite shell stabilizes the droplets compared to microdroplets alone. For example, individual microdroplets easily merged to larger droplets in the absence of the DNA-SiNP nanocomposite shell. As such, the collected hollow spheres of DNA-SiNP nanocomposite showed a relatively uniform diameter (see Figure 4a, b, main manuscript) and, in particular, they displayed a substantial long-term stability under static storage conditions (≥ 3 d). Conversely, the microdroplets lacking the DNA-SiNP nanocomposite shell shrank, collapsed or changed their shapes randomly within a short time period (typically <12 h).

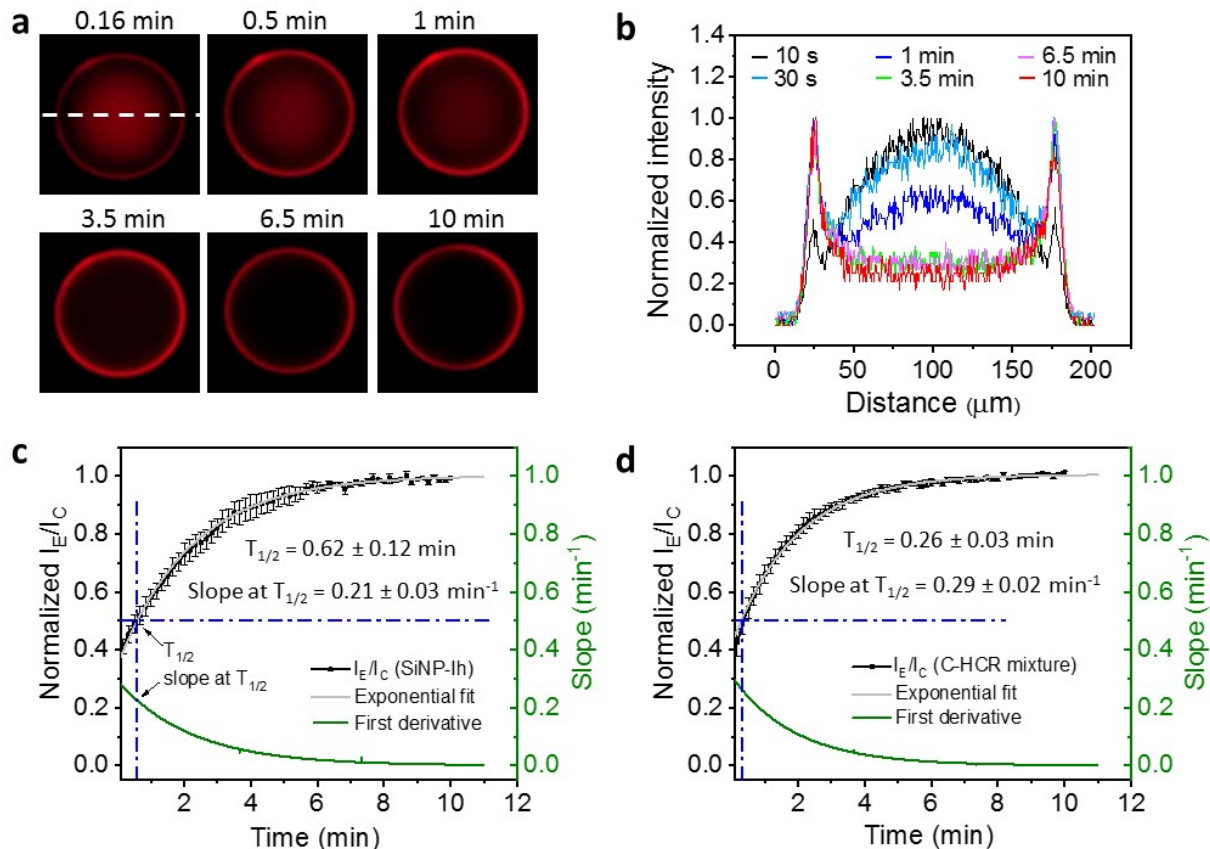


Figure S9. Segregation kinetics of SiNP inside DOTAP W/O droplets. **a**, Representative real-time fluorescence images of the SiNP-Ih suspension in DOTAP W/O droplets at different time points and **(b)** corresponding fluorescence intensity profiles recorded along the dashed line. **c**, Plotting of fluorescence intensity at the edge of the droplet (I_E) to the expense of intensity in the center (I_C) against time for **(c)** pure SiNP-Ih and **(d)** a C-HCR mixture of H1/H2 and prepolymerized SiNP-Ih, prepared by h1/h2-mediated linear HCR (see Figure S3). The slope at $T_{1/2}$ was plotted in **(c)** and **(d)** to illustrate the diffusion rate of the SiNP. A lower diffusion rate was found for the pure SiNP-Ih (0.21 min^{-1} , in c) as compared to the SiNP-Ih in C-HCR reaction mixture (0.29 min^{-1} , in d). These results indicate that a faster assembly process occurs in the presence of the C-HCR reaction mixture, presumably due to the higher concentration of DNA in these W/O droplets.

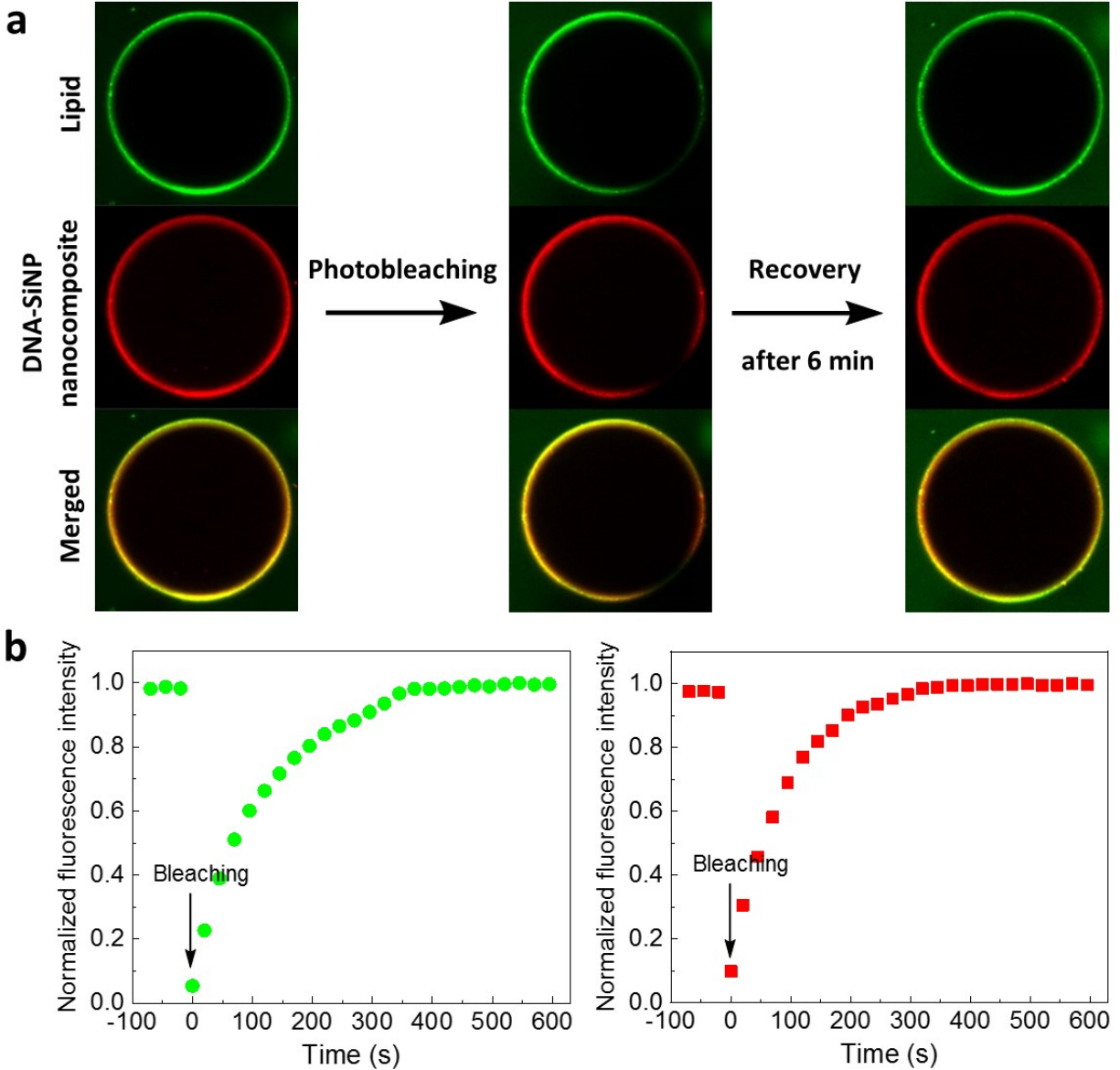


Figure S10. FRAP analysis of DOTAP W/O droplets containing SiNP-Ic. **a**, Representative fluorescence images of DOTAP W/O droplet before and after photobleaching. **b**, FRAP curves of lipid membrane (green dots) and the DNA-SiNP shell bearing SiNP-Ic (red square). Note that, the fluorescence intensities of the lipid membrane and SiNP-Ic recovered at ~6 min and ~5.5 min post bleaching, respectively. Also note that SiNP-Ic were treated similar as SiNP-Ih used for the experiments shown in Figure 3c, main text. I.e., SiNP-Ic were subjected to “prepolymerization” by h1/h2-mediated linear HCR and then mixed with the H1/H2 hairpins before encapsulation into the W/O droplets.

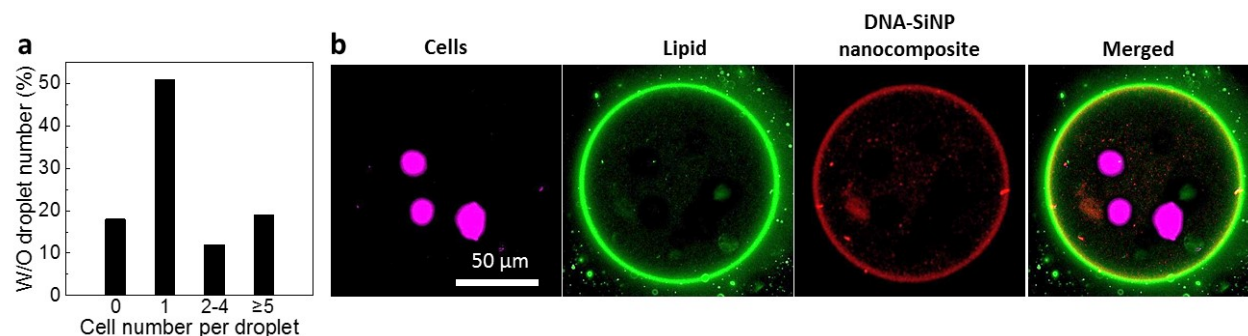


Figure S11. Analysis of the cells encapsulated within the DNA-SiNP nanocomposite microcontainers. **a**, Statistical analysis of the number of cells encapsulated inside the hollow-sphere microcontainers. Note that 2×10^6 cells per mL medium were used to ensure that individual droplets were loaded with only few cells. **b**, and fluorescence images of microcontainers with CHO-S cells. Fluorescence images of a cell-loaded microcontainer bearing 3 CHO-S cells. Lipids are shown in green, DNA-SiNP composite in red and cells, pre-stained with Calcein AM, in violet.

References

- [1] X. D. Wang, K. S. Rabe, I. Ahmed and C. M. Niemeyer, *Adv. Mater.* **2015**, *27*, 7945–7950.
- [2] A. Leidner, S. Weigel, J. Bauer, J. Reiber, A. Angelin, M. Grösche, T. Scharnweber and C. M. Niemeyer, *Adv. Funct. Mater.* **2018**, *28*, 1707572.
- [3] M. Grosche, A. E. Zoheir, J. Stegmaier, R. Mikut, D. Mager, J. G. Korvink, K. S. Rabe and C. M. Niemeyer, *Small* **2019**, *15*, e1901956.
- [4] J. Wang, J. Chao, H. Liu, S. Su, L. Wang, W. Huang, I. Willner and C. Fan, *Angew. Chem. Int. Ed.* **2017**, *56*, 2171-2175.